Liu, Fupeng; Peng, Chao; Wilson, Benjamin P.; Lundström, Mari

Oxalic acid recovery from high iron oxalate waste solution by a combination of ultrasound-assisted conversion and cooling crystallization

Published in:
ACS Sustainable Chemistry and Engineering

DOI:
10.1021/acssuschemeng.9b04351

Published: 01/01/2019

Document Version
Publisher's PDF, also known as Version of record

ACS Sustainable Chemistry & Engineering

Research Article

Cite This: ACS Sustainable Chem. Eng. 2019, 7, 17372−17378

pubs.acs.org/journal/ascecg

Oxalic Acid Recovery from High Iron Oxalate Waste Solution by a Combination of Ultrasound-Assisted Conversion and Cooling Crystallization

Fupeng Liu,[†,‡] Chao Peng,[‡] Benjamin P. Wilson,[‡] and Mari Lundström*[,‡]

[†]Institute of Engineering Research, Jiangxi University of Science and Technology, Ganzhou 341000, China

[‡]Hydrometallurgy and Corrosion, Department of Chemical and Metallurgical Engineering (CMET), School of Chemical Engineering, Aalto University, P.O. Box 12200, FI-00076 Aalto, Finland

ABSTRACT: To achieve the global goals related to renewable energy and responsible production, technologies that ensure the circular economy of metals and chemicals in recycling processes are a necessity. The recycling of spent Nd−Fe−B magnets typically results in rare-earth element (REE)-free wastewater that has a high ferric ion concentration as well as oxalate groups and for which there are only a few economically viable methods for disposal or reuse. The current research provides a new approach for the effective recovery of oxalic acid, and the results suggest that during the initial oxalate group separation stage, >99% of oxalate ions can be precipitated as ferrous oxalate ($FeC_2O_4{\cdot}2H_2O$) by an ultrasound-assisted iron powder replacement method (Fe/Fe(III) = 2, $t_{u/s}$ = 5 min, T = 50 °C). Subsequently, almost all $FeC_2O_4{\cdot}2H_2O$ was dissolved using 6 mol/L HCl (T = 65 °C, t = 5 min) and the dissolved oxalates were found to mainly exist in the form of $H_2C_2O_4$. Furthermore, over 80% of the oxalic acid was recovered via crystallization by cooling the oxalate containing HCl solution to 5 °C. After oxalic acid crystallization, the residual raffinate acid solution can then be recirculated back to the ferrous oxalate leaching stage, to decrease any oxalic acid losses. This treatment protocol for high-iron REE-free solution not only avoids the potential harm to the environment due to the wastewater but also significantly improves the circular economy of chemicals in the typical utilization in permanent magnet recycling processes.

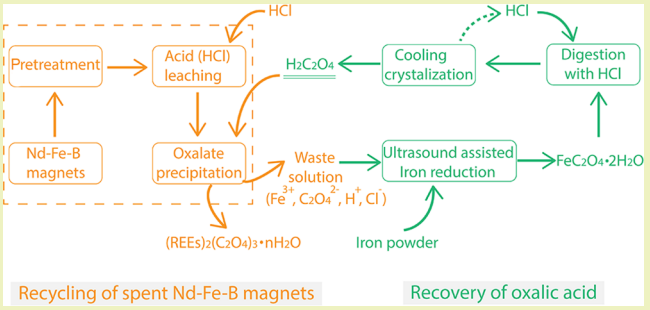

KEYWORDS: *oxalic acid recycling, ultrasound-assisted precipitation, Nd−Fe−B magnets, cooling crystallization*

INTRODUCTION

The most important rare-earth permanent magnets are composed of Nd−Fe−B alloys, which due to their excellent magnetic characteristics, compactness, and lightweight are widely utilized in automobiles, wind turbines, computer hard disk drives, electronic vehicles, etc.[1] A recent report has found that the production of Nd−Fe−B magnets has nearly doubled within the past 5 years, and by 2020, it is predicted that around 130 kt of Nd−Fe−B magnets, which would require 35 kt of REEs or approximately 22% of the global supply, will be produced.[2] Consequently, when the limited lifetime of, for example, 2−3 years of consumer electronics and 20−30 years of wind turbines are considered, a significant amount of end-of-life magnets will become available in the near future[3,4] providing a significant secondary resource for REE production. In addition, a further 20−30% of the magnet raw material is lost as waste during the shaping, surface treatment, and magnetization of the final Nd−Fe−B magnet products.[5,6] As the rare-earth content in Nd−Fe−B permanent magnets is more than 30%, the recycling of Nd−Fe−B magnets has attracted significant global interest from both academia and industry.[7−9]

Currently, one of the main industrial processes for the recovery of REEs from spent Nd−Fe−B magnets involves the oxidative roasting of the spent magnet material, acidic decomposition, and the precipitation of REEs in the form of REE oxalates ($(RE)_2(C_2O_4)_3{\cdot}nH_2O$).[6,9] Nevertheless, a previous study has found that >50% of the Fe dissolved during this process exists in the form of Fe(II) and that its presence within the oxalate solution can result in the formation of the FeC_2O_4 precipitate that decreases the purity of the resultant REE products.[10] As a result, to improve the quality of the REE oxalate products, additional iron removal steps are proposed to be performed prior to the REE precipitation. A traditional process for iron removal involves neutralization precipitation after ferrous ion oxidation. This methodology effectively removes almost all iron (Fe(II) and Fe(III)) present, although between 20 and 30% of REE losses by coprecipitation or mechanical entrainment have been observed.[11] Some other alternative methods such as electro-

Received: July 27, 2019
Revised: September 14, 2019
Published: September 19, 2019

Table 1. Chemical Composition of the Solution (mg/L) Used as Raw Material in the Study

elements	Fe	Co	B	Nd	Pr	Gd	Dy	Ho	$(C_2O_4)^{2-}$
concentration	10,200	500	690	23	15	8	11	8	50,000

chemical oxidation precipitation and solvent extraction by trihexyl(tetradecyl)phosphonium (Cyphos IL101) or tri(octyldecyl) amine (N235) have also been developed,[12,13] and the iron can be effectively separated from REEs. Nonetheless, industrial utilization of these iron removal methods would complicate the production process leading to an increase in production costs and investment required for infrastructure.

In contrast, one industrially feasible method is to selectively extract REEs from high-concentration iron solutions. First, the Fe(II) ions in the acid leachate are oxidized to Fe(III), which have a minor effect on REE product purity,[10] before the REEs are selectively precipitated as REE oxalate products, to leave the ferric iron in the raffinate. However, the induced increase in ferric ion concentration results in increased oxalic acid consumption due to strong complexation between oxalate and Fe(III) ions.[14] REE precipitation efficiency has been suggested to reach 90% but only in the presence of a high oxalic acid excess, n(oxalic acid)/n(REEs) > 3,[10] which means that high REE precipitation efficiency generates large quantities of high Fe oxalic acid wastewater. Additionally, when the high price of oxalic acid is taken into consideration, it is critical that methodologies that both separate and recover oxalate ions from the REE-free solution are developed to improve the economic and environmental aspects of Nd−Fe−B magnet waste recycling.

Conventionally, calcium oxalate precipitation is used to recover the residual oxalic acids from the wastewater; however, this process generates significant amounts of calcium sulfate residues and a recovery efficiency of <80%.[15] To avoid the potential hazards caused by waste residues and to improve oxalic acid recovery, a number of solvent extraction methods have also been developed. For example, tributyl phosphate (TBP) and di(1-methylheptyl)methylphosphonate (P350) both have been found to be an effective solvent extractant for the extraction of oxalic acid from low iron aqueous solutions.[16−18] However, for the solutions containing high ferric ion levels (e.g., above 10 g/L Fe), both TBP and P350 have challenges due to the strong complexation between oxalate and Fe(III) ions, with only ∼60% of oxalic acid extracted from such high iron oxalate solution under optimal conditions.

To improve the oxalic acid recovery from the high Fe(III) solution, it is suggested to first destroy the stable complex structure formed by the oxalate group and Fe(III).[19] One promising alternative method is by iron reduction precipitation through which Fe(III) ions were reduced into Fe(II) and then form the precipitate of FeC_2O_4 ($K_{sp} = 3.2 \times 10^{-7}$) with oxalate groups. Nevertheless, it was found that more than three times the stoichiometry of iron scraps was required to completely reduce Fe(III) into Fe(II) due to the formation of a passive $FeC_2O_4{\cdot}2H_2O$ layer on the surface of the iron scraps that prevents the reduction reaction of Fe(III).[19] Additionally, there is limited information available for the further treatment of the produced ferrous oxalate precipitates, that is, the recovery of oxalate ions from $FeC_2O_4{\cdot}2H_2O$ precipitates. As a result, in this study, we proposed a method to treat the high Fe oxalic acid-bearing waste solution by iron reduction precipitation with the assistance of ultrasound. The ultrasonic cavitation effect was supposed to be beneficial for the breakdown of the passive surface layer ($FeC_2O_4{\cdot}2H_2O$) between products and solution,[20,21] which has been widely employed in the hydrometallurgical processes over the past decades.[22,23] After the precipitation of oxalate ions, acid dissolution with HCl followed by cooling crystallization was performed to recover $H_2C_2O_4$ that can be reused for the precipitation of REEs. The residual solution (rich in HCl and $FeCl_2$) after the crystallization of $H_2C_2O_4$ can be utilized for the acid dissolution of $FeC_2O_4{\cdot}2H_2O$ precipitates. The behavior of iron and oxalate ions during each process step was investigated in detail to allow process optimization and increase the possibilities for industrial application.

EXPERIMENTAL SECTION

Reagents and Solutions. Residual pregnant leach solution (PLS)—rich in Fe (10 g/L) and $(C_2O_4)^{2-}$ (50 g/L)—after REE precipitation from Nd−Fe−B leaching solution was used as the input for the oxalic acid recovery experiments, and a more detailed solution composition is outlined in Table 1. Prior to REE precipitation, Fe(II) was oxidized into Fe(III) in the Nd−Fe−B leaching process to avoid the formation of the FeC_2O_4 precipitate ($K_{sp} = 4 \times 10^{-11}$); therefore, Fe is assumed to exist in the higher valance state.[10] The molar ratio of Fe and $(C_2O_4)^{2-}$ in the solution is nearly 1:3, which suggests the presence of the $Fe(C_2O_4)_3^{3-}$ complex. All the chemicals used in this study were of analytical grade and deionized water was used in all experiments.

Characterization and Analysis. The concentrations of Fe (total), Co, B, and REEs were determined by inductively coupled plasma-optical emission spectroscopy (ICP-OES, PerkinElmer Optima 7100 DV, USA). The Fe(II) concentration in the REE-free solution was analyzed by the potassium dichromate method. In contrast, the Fe(III) concentrations in solution were analyzed by a precipitation separation—EDTA titration method.[24] The main mineral phases within the products of ferrous oxalate and oxalic acid were identified by XRD (PANalytical X'Pert Pro Powder, Almelo, the Netherlands) using a Co Kα radiation source with a 40 kV acceleration potential and a current of 40 mA. XRD diffractograms were analyzed by HighScore 4.0 Plus software. The morphology and size of the oxalate precipitates were determined by SEM (A LEO 1450, Carl Zeiss Microscopy GmbH, Jena, Germany). The concentration of the oxalate group when there was no Cl^- in solution was analyzed using a potassium permanganate titration method, whereas the amount of oxalate in hydrochloric acid solution was ascertained via a total organic carbon analyzer (TOC, TOC-V CPH, Shimadzu, Japan). The species and structure of the oxalate group in the ferrous oxalate leach solution was confirmed by horizontal attenuated total reflectance Fourier transform infrared (HATR-FTIR) spectroscopy (Nicolet IS10, Thermo Scientific, USA).

Experimental Procedure. *Ultrasound-Assisted Precipitation of Oxalate Ions.* Given that iron exists as a soluble $Fe(C_2O_4)_3^{3-}$ complex, iron powders were first added to reduce the Fe(III) to Fe(II), which then subsequently react with oxalate ions to form FeC_2O_4 precipitates, leading to the extraction of oxalate ions from the processed solution. Ultrasonic power (Ultrasonic Cleaner, Elmasonic S15H) was utilized to promote the distribution of iron powder and enhance the Fe(III) reduction reaction. Sonication power was set at 150 W and a water bath (Thermo Haake, DC10) was utilized to achieve a high recovery efficiency of the oxalate via the oxalate precipitation reaction. Parameters including the Fe dosage (mole ratio of Fe/Fe(III) = 1−2.5), sonication time ($t_{u/s}$ = 0−10 min), reaction temperature (T = 30−90 °C), and reaction time (t_r = 10−120 min) in the water bath were optimized to achieve the high oxalate ion

DOI: 10.1021/acssuschemeng.9b04351
ACS Sustainable Chem. Eng. 2019, 7, 17372−17378

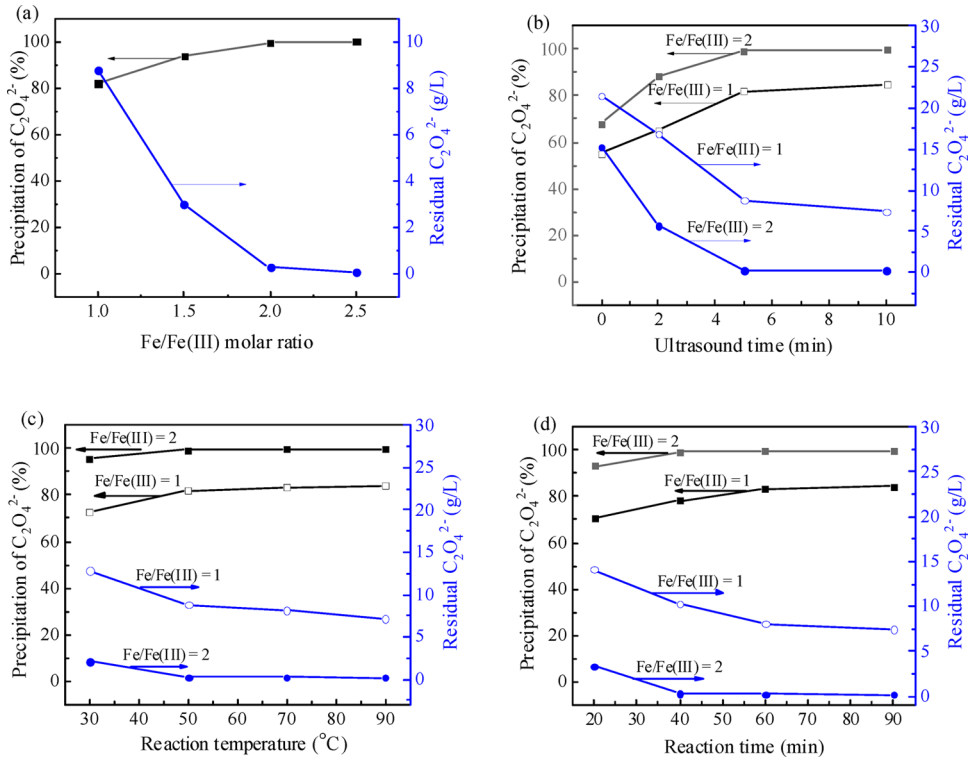

Figure 1. Precipitation of oxalate ions as a function of (a) Fe/Fe(III) molar ratios ($t_{u/s}$ = 5 min, T = 50 °C, t_r = 40 min), (b) ultrasound time (T = 50 °C, t_r = 40 min), (c) reaction temperature ($t_{u/s}$ = 5 min, t_r = 40 min), and (d) reaction time in water bath ($t_{u/s}$ = 5 min, T = 50 °C).

extraction. After a predetermined reaction time, FeC_2O_4 precipitates were filtered and dried at 95 °C for 12 h. The contents of ferric iron and ferrous iron, as well as the oxalate group, in the solution before and after the reduction step were analyzed.

Acid Dissolution of Ferrous Oxalate. Dissolution of the FeC_2O_4 precipitates obtained was investigated in different concentrations of hydrochloric acid solution. The experiments were conducted in 300 mL round-bottom flasks, with magnetic stirring at 300 rpm with temperature controlled by a water bath (Thermo Haake, DC10). In each run, 200 mL of hydrochloric acid solution was put into a flask and then heated to a preset temperature, before the addition of ferrous oxalate precipitates. After a defined leaching time, the resultant slurry was filtered to obtain any residual oxalate precipitates and a filtrate. The decomposition of ferrous oxalates was determined as a function of dissolution time (5−120 min), hydrochloric acid concentration (1−9 mol/L), and liquid-to-solid ratio (5−15 mL/g). The dissolution efficiency (%E) of the ferrous oxalate is defined as

$$\%E = (C_M \times V)/(m \times w) \times 100\% \quad (1)$$

where C_M is the concentration of iron in the leachate, V is the volume of dissolution solution, m is the mass of input oxalate precipitates (g), and w is the content of iron in oxalate precipitates.

Crystallization of $H_2C_2O_4$. After the acid leaching of ferrous oxalate precipitates ($FeC_2O_4{\cdot}2H_2O$) at optimum conditions, 20 mL of the leachate was added in a 50 mL cylindrical reactor without stirring and then refrigerated at a temperature between 0 and 10 °C. After the required reaction time, the suspension was filtered immediately and any resultant oxalic acid crystals were dried at 50 °C for 48 h. The volume of the solution after crystallization was recorded and the oxalic acid concentration was analyzed by measuring the total organic carbon (TOC) concentration. The precipitation efficiency of oxalic acid (%P) was defined as

$$\%P = [(1 - (V_1 \times C_1)/(V_0 \times C_0)] \times 100\% \quad (2)$$

where C_0 and C_1 represent the initial and final concentrations of oxalic acid before and after the crystallization procedure, respectively, and V_0 and V_1 are the volumes of solution before and after crystallization, respectively.

RESULTS AND DISCUSSION

Ultrasound-Assisted Precipitation of Oxalate Ions. In this study, the ultrasound-assisted iron powder reduction process was adopted to extract the oxalate ions by forming the $FeC_2O_4{\cdot}2H_2O$ precipitate. The main reactions can be described as follows:

$$2Fe(C_2O_4)_3^{3-} + Fe + 6H_2O \rightarrow 3FeC_2O_4{\cdot}2H_2O + 3C_2O_4^{2-}$$
$$\log K_{(298.15)} = 19.20 \quad (3)$$

$$Fe + 2H^+ \rightarrow Fe^{2+} + H_2(g)$$
$$\log K_{(298.15)} = 16.03 \quad (4)$$

$$Fe^{2+} + C_2O_4^{2-} + 2H_2O \rightarrow 2FeC_2O_4{\cdot}2H_2O$$
$$\log K_{(298.15)} = 6.47 \quad (5)$$

Effects of principal factors (molar ratios of Fe/Fe(III), ultrasound time, reaction time, and temperature) on the precipitation of oxalate ions were examined with an ultrasound power of 150 W. The results shown in Figure 1a,b indicate that the oxalate ion removal ratio is strongly depended on the Fe/Fe(III) molar ratio and sonication time. As can be seen, the precipitation of oxalate ions increases from approximately 80 to 99% as the Fe/Fe(III) molar ratio increased from 1 to above 2. The corresponding concentration of residual oxalate groups ($C_2O_4^{2-}$) decreases from approximately 9 to 0.06 g/L. In addition, it can be observed from Figure 1b that precipitation of oxalate ions increases by approximately 30% with the application of an ultrasound power of 150 W for only 5 min at Fe/Fe(III) ratios of 1 and 2. This obvious enhancement with

DOI: 10.1021/acssuschemeng.9b04351
ACS Sustainable Chem. Eng. 2019, 7, 17372−17378

ultrasound results from the facilitated mass transfer through the product layer induced by the ultrasonic cavitation.[22] Over the investigated range of ultrasound treatment (shown in Figure 1b), the precipitation of oxalate ions at an Fe/Fe(III) molar ratio of 2 remains 10−20% higher than that obtained when Fe/Fe(III) = 1. By contrast, other parameters like reaction temperature (Figure 1c) and reaction time (Figure 1d) were observed to have only a limited effect on the oxalate ion precipitation. The precipitation of oxalate ions was found to vary by only approximately 5% under the experimental reaction conditions (reaction temperature and time) studied, and the optimum results can be achieved at 50 °C for 40 min after ultrasound treatment.

To sum up, above 99% of oxalate ions can be precipitated through this ultrasound-assisted iron reduction process (Fe/Fe(III) mole ratio of 2 and sonication (150 W and 5 min) at 50 °C for 40 min), resulting a precipitate in the form of $FeC_2O_4{\cdot}2H_2O$ (shown in Figure 2).

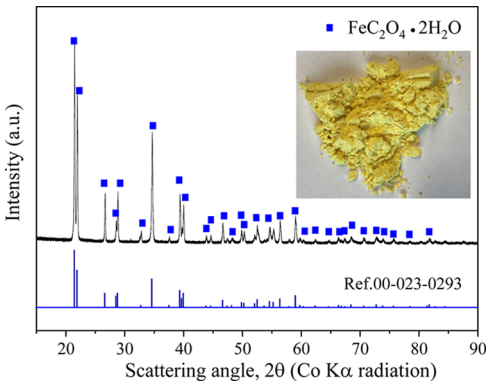

Figure 2. X-ray diffraction pattern of the residue after iron removal (Fe/Fe(III) = 2, ultrasound power = 150 W, $t_{u/s}$ = 5 min, T = 50 °C, t_r = 40 min).

Decomposition of $FeC_2O_4{\cdot}2H_2O$ Using HCl. Decomposition of the $FeC_2O_4{\cdot}2H_2O$ produced as a function of HCl concentration was investigated at 65 °C with a solid-to-liquid (S/L) ratio of 100 g/L for 5 h. The results displayed in Figure 3a show that dissolution of ferrous oxalate increases substantially with the increase in HCl concentration from 1 to 4 mol/L and that a complete decomposition of $FeC_2O_4{\cdot}2H_2O$ was achieved when HCl concentrations are >4 mol/L. In addition, it is also clear that the associated dissolution kinetics is faster with higher HCl concentrations. For example, with a 4 mol/L HCl solution, it takes 5 h to dissolve nearly 100% $FeC_2O_4{\cdot}2H_2O$ (Figure 3a), whereas when 5 mol/L HCl was used, completed dissolution was achieved within 5 min (Figure 3b). Figure 3b also shows that an increase in the reaction temperature was conducive to the dissolution of $FeC_2O_4{\cdot}2H_2O$ as decomposition of the ferrous oxalate increased from 45% to almost 100% when the temperature was changed from 25 to 65 °C.

The influence of the solid-to-liquid (S/L) ratio was studied at 5 and 6 mol/L HCl (T = 65 °C, t = 5 min) and the findings demonstrate that the leaching efficiency of FeC_2O_4 decreased significantly with increasing S/L ratios in both 5 and 6 mol/L HCl (Figure 3c). When S/L = 200 g/L, leaching efficiency of FeC_2O_4 was only 54% with 6 mol/L HCl, whereas with an S/L ratio of 150 g/L, almost all $FeC_2O_4{\cdot}2H_2O$ could be dissolved within 5 min as shown in Figure 3c. The leach solution was obtained with 70 g/L oxalate group at selected optimum conditions (S/L = 150 g/L, HCl = 6 mol/L, T = 65 °C, t = 5 min). An FTIR spectrum of the leaching solution obtained was also measured and a comparison was performed with a pure oxalic acid solid reference (Figure 3d). The results clearly show that carbonyl bands related to (COO^- ν_{as}) asymmetric stretching vibrations and corresponding symmetric stretches (COO^- ν_s) can be clearly identified at ∼1630 and ∼1380 cm^{-1}. In addition, the band at 1270 cm^{-1} represents the bending stretches of C−OH groups, which indicates the presence of oxalic acid ($H_2C_2O_4$) within the acid leaching solution. Overall, high acidity was found to promote the release of oxalate ion from ferrous oxalates and the formation of free oxalic acid in solution, which facilitates the subsequent crystallization of oxalic acid.

Recovery of $H_2C_2O_4$ by Cooling Crystallization. After decomposition of ferrous oxalate with HCl > 5 mol/L, the oxalate group is predominantly in the form of $H_2C_2O_4$ rather than $HC_2O_4^-$ or $C_2O_4^{2-}$—the first and second ionization constants of $H_2C_2O_4$ are 5.9 × 10^{-2} and 6.4 × 10^{-5}, respectively—which indicates that the ferrous oxalate is decomposed to $FeCl_2$ and $H_2C_2O_4$ in concentrated hydrochloric acid solution. As the recovery of oxalic acid by cooling crystallization is determined by the solubility of oxalic acid at different acid concentrations, it is necessary to first study the dissolution behavior of oxalic acid in HCl at different freezing temperatures. The synthetic solution (70 g/L $H_2C_2O_4$) with different concentrations of HCl was prepared to first investigate the crystallization behavior of oxalic acid. Figure 4a shows the effects of HCl concentration on the recovery of oxalic acid. These results indicate that the solubility of oxalic acid decreases gradually to a minimum of about 15 g/L when HCl = 6 mol/L after which further increases in HCl concentration a steady enhancement of solubility up to a local maximum of 38 g/L at HCl = 9 mol/L. The $H_2C_2O_4$ concentration in the residual solution, as shown in Figure 4a, also decreases with a reduction in the freezing temperature from 10 to 5 °C, whereas there is no obvious change when temperature is further reduced from 5 to 0 °C. Based on these results, conditions of 6 mol/L HCl concentration in REE-free solution and a cooling temperature of 5 °C were selected for the following crystallization of oxalic acid, and Figure 4b illustrates that almost 79% of oxalic acid can be recovered within 2 h under these optimized conditions. As shown from Figure 5, higher hydrochloric acid concentrations promote the formation and growth of oxalic acid crystals, especially in terms of increased $H_2C_2O_4$ crystal size—compare the transition from 4 to 6 mol/L, for example.

The cooling crystallization of the real leaching solution, produced with different HCl concentrations (4−9 mol/L) and S/L = 100 g/L, is displayed in Figure 6a. Recovery of oxalic acid was found to increase slightly with increasing HCl concentration (i.e., final concentration after leaching) from 78 (2.5 mol/L HCl) to 82% (6.5 mol/L HCl). This also leads to a reciprocal decrease of oxalic acid in the residual solution from 14.5 to 12.5 g/L, and the behavior correlates well with the findings previously observed with the synthetic solutions (Figure 4a).

Overall, the results clearly demonstrate that around 80%, oxalic acid with a good crystallization (Figure 6b) could be recovered from the acid leach solution of ferrous oxalate. The residual solution following freeze crystallization was found to comprise of approximately 0.15 mol/L $H_2C_2O_4$, 3.5 mol/L

DOI: 10.1021/acssuschemeng.9b04351
ACS Sustainable Chem. Eng. 2019, 7, 17372−17378

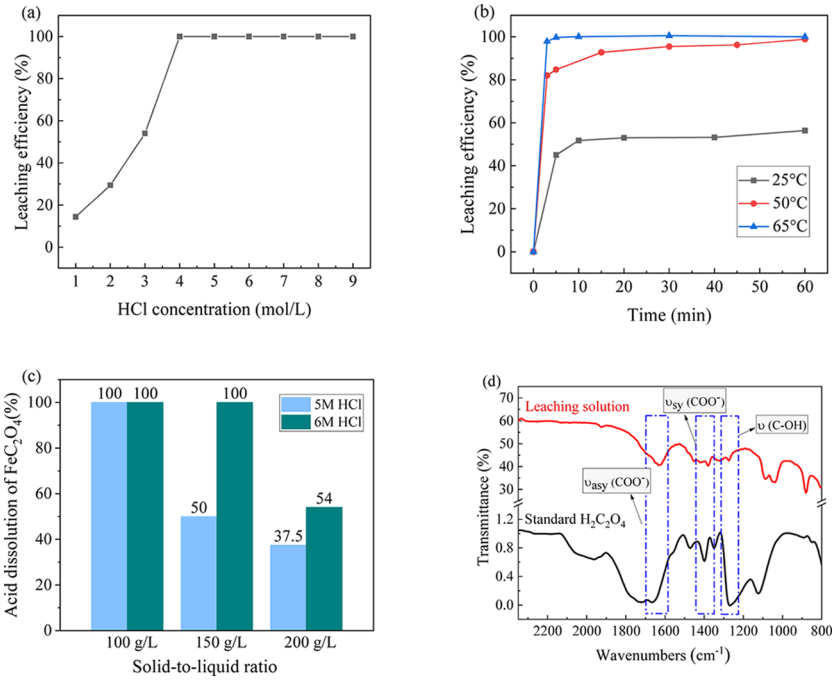

Figure 3. Acid leaching efficiency of $Fe_2C_2O_4{\cdot}2H_2O$ as a function of (a) HCl concentration (S/L = 100 g/L, T = 65 °C, t = 5 h), (b) leaching time (S/L = 100 g/L, T = 65 °C, HCl = 5 mol/L), (c) liquid-to-solid ratios (T = 65 °C, t = 5 min), and (d) the FTIR spectra of pure oxalic acid and the acid leaching solution.

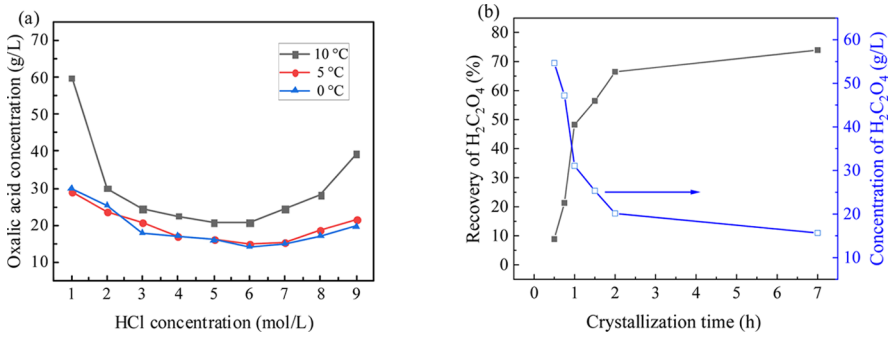

Figure 4. Recovery of oxalic acid as a function of (a) HCl concentration and temperature (t = 5 h) and (b) crystallization time (T = 5 °C, HCl = 6 mol/L).

HCl, and 0.7 mol/L $FeCl_2$, and this raffinate acid solution is fully recyclable to the ferrous oxalate leaching stage, which then allows the residual $H_2C_2O_4$ to be recirculated to the crystallization process. Furthermore, when the effect of $FeCl_2$ solubility on the dissolution of $FeC_2O_4{\cdot}2H_2O$ is taken into account, the ferrous chloride can also be recovered by evaporation crystallization once it attains a suitable concentration level.

Flowsheet Development. From the results of the experiments detailed here, it is possible to develop a new process to recover oxalate ions from Nd−Fe−B leaching solutions. The process is based on the combination of ultrasound-assisted ferrous iron precipitation, decomposition of $FeC_2O_4{\cdot}2H_2O$, and cooling crystallization of $H_2C_2O_4$. Moreover, as an excess of iron can accumulate during the process, an evaporation crystallization stage can be included for $FeCl_2$ removal. The low-iron HCl solution obtained from the crystallization of $H_2C_2O_4$ or $FeCl_2$ can be circulated for use as a leaching agent for the decomposition of $FeC_2O_4{\cdot}2H_2O$. Nevertheless, it is clear that during the whole process, an excess of HCl would be required that would accumulate over time, although this excess HCl can be further converted into ferrous chloride with the addition of iron powder or separated from the solution by vacuum evaporation.

Overall, the application of this new, low energy, and high recovery efficiency process shown in Figure 7 on an industrial scale could significantly improve the recovery of oxalic acid from residual (REE-free) acidic leach waste solutions generated by spent Nd−Fe−B magnet recycling. Furthermore, in addition to the environmental benefits of waste reduction, the utilization of this oxalic acid within the recycling process will have a positive impact on the operational costs associated with REE recovery.

CONCLUSIONS

This research outlines a novel process (Figure 7) for the effective recovery of oxalic acid from the wastewater produced by the recycling of spent Nd−Fe−B permanent magnets. This contributes to the improved recyclability of permanent

DOI: 10.1021/acssuschemeng.9b04351
ACS Sustainable Chem. Eng. 2019, 7, 17372−17378

Figure 5. Morphology of oxalic acid products at different HCl concentrations (t = 2 h, T = 5 °C).

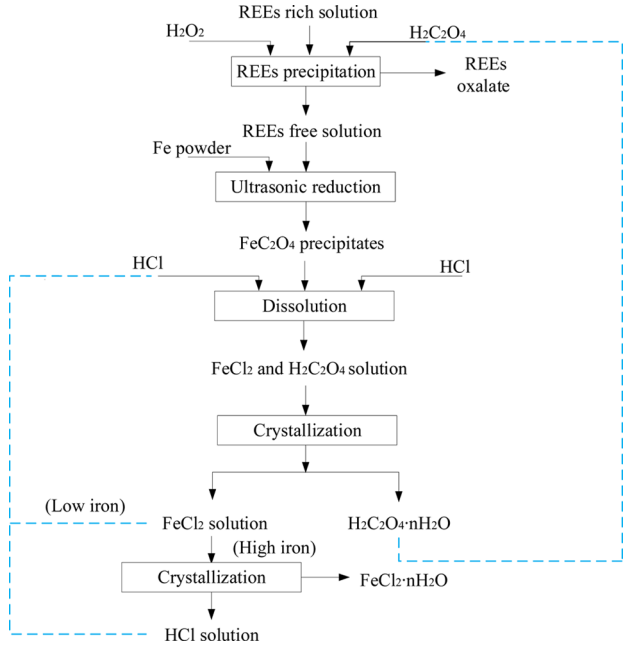

Figure 7. Flow sheet proposed for the recovery of oxalic acid and iron from high iron oxalate wastewater produced from spent Nd−Fe−B permanent magnet recycling.

(Nd−Fe−B) magnets as well as a reduction in the chemicals and waste associated with the recycling process.

The results suggest that the oxalate ion removal by the ultrasound-assisted iron powder method is strongly dependent on the Fe/Fe(III) molar ratio as well as total sonication time. Under the optimum conditions, more than 99% of oxalate ions could be recovered and the $FeC_2O_4{\cdot}2H_2O$ products obtained were readily decomposed (HCl > 6 mol/L) to produce a solution containing oxalates in the form of $H_2C_2O_4$. The minimum solubility of oxalic acid was found at 6 mol/L HCl solution. Oxalic acid recovery was conducted by freeze crystallization and >80% recovery was achieved at an optimum temperature of 5 °C. These findings indicate that the approach outlined here offers an efficient method for oxalic acid recovery and the direct recirculation of any remaining acid and oxalates back to the ferrous oxalate leaching stage. Overall, industrial utilization of this low energy and high recovery efficiency process could both significantly reduce the level of waste and enhance the process economics associated with spent Nd−Fe−B magnet recycling.

AUTHOR INFORMATION

Corresponding Author

*E-mail: mari.lundstrom@aalto.fi.

ORCID

Chao Peng: 0000-0003-2347-2556

Benjamin P. Wilson: 0000-0002-2874-6475

Notes

The authors declare no competing financial interest.

ACKNOWLEDGMENTS

The authors would also like to acknowledge the financial support from the National Nature Science Foundation of China (no.51804141) as well as the Science and Technology Project of the Education Department of Jiangxi Province (GJJ170533). The authors also acknowledge the HYMAG project (SL/84/04.03.00.0400/2017) funded by the Regional Council of Satakunta, AIKO funding. This paper also made use of the Academy of Finland's RawMatTERS Finland Infrastructure (RAMI) based at Aalto University.

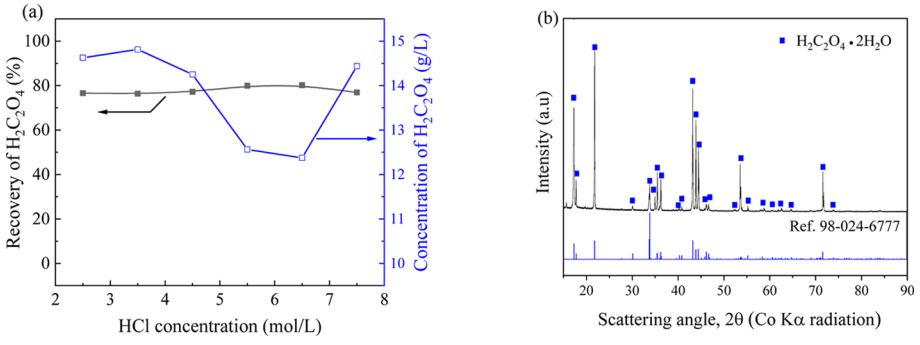

Figure 6. (a) Recovery of oxalic acid ($H_2C_2O_4$) from the practical leach solution (initial [$H_2C_2O_4$] = 70 g/L, T = 5 °C, t = 2 h) and (b) XRD pattern of the oxalic acid produced.

DOI: 10.1021/acssuschemeng.9b04351
ACS Sustainable Chem. Eng. 2019, 7, 17372−17378

REFERENCES

(1) Miura, K.; Itoh, M.; Machida, K.-I. Extraction and Recovery Characteristics of Fe Element from Nd-Fe-B Sintered Magnet Powder Scrap by Carbonylation. *J. Alloys Compd.* **2008**, *466*, 228−232.

(2) Yang, Y.; Walton, A.; Sheridan, R.; Güth, K.; Gauß, R.; Gutfleisch, O.; Buchert, M.; Steenari, B.-M.; Van Gerven, T.; Jones, P. T.; et al. REE Recovery from End-of-Life NdFeB Permanent Magnet Scrap: A Critical Review. *J. Sustainable Metallurgy* **2017**, *3*, 122−149.

(3) Du, X.; Graedel, T. E. Global In-Use Stocks of the Rare Earth Elements: A First Estimate. *Environ. Sci. Technol.* **2011**, *45*, 4096−4101.

(4) Tunsu, C. Hydrometallurgy in the Recycling of Spent NdFeB Permanent Magnets. In *Waste Electrical and Electronic Equipment Recycling*; Vegliò, F., Birloaga, I., Eds.; Woodhead Publishing: Cambridge, MA, 2018, pp 175−211.

(5) Horikawa, T.; Miura, K.; Itoh, M.; Machida, K. Effective Recycling for Nd−Fe−B Sintered Magnet Scraps. *J. Alloys Compd.* **2006**, *408-412*, 1386−1390.

(6) Kumari, A.; Sinha, M. K.; Pramanik, S.; Sahu, S. K. Recovery of Rare Earths from Spent NdFeB Magnets of Wind Turbine: Leaching and Kinetic Aspects. *Waste Manage.* **2018**, *75*, 486−498.

(7) Önal, M. A. R.; Aktan, E.; Borra, C. R.; Blanpain, B.; Van Gerven, T.; Guo, M. Recycling of NdFeB magnets using nitration, calcination and water leaching for REE recovery. *Hydrometallurgy* **2017**, *167*, 115−123.

(8) Firdaus, M.; Rhamdhani, M. A.; Rankin, W. J.; Pownceby, M.; Webster, N. A. S.; D'Angelo, A. M.; McGregor, K. High temperature oxidation of rare earth permanent magnets. Part 1 − Microstructure evolution and general mechanism. *Corros. Sci.* **2018**, *133*, 374−385.

(9) Vander Hoogerstraete, T.; Blanpain, B.; Van Gerven, T.; Binnemans, K. From NdFeB magnets towards the rare-earth oxides: a recycling process consuming only oxalic acid. *RSC Adv.* **2014**, *4*, 64099−64111.

(10) Venkatesan, P.; Sun, Z. H. I.; Sietsma, J.; Yang, Y. An Environmentally Friendly Electro-Oxidative Approach to Recover Valuable Elements from NdFeB Magnet Waste. *Sep. Purif. Technol.* **2018**, *191*, 384−391.

(11) Rabatho, J. P.; Tongamp, W.; Takasaki, Y.; Haga, K.; Shibayama, A. Recovery of Nd and Dy from rare earth magnetic waste sludge by hydrometallurgical process. *J. Mater. Cycles Waste Manage.* **2013**, *15*, 171−178.

(12) Venkatesan, P.; Vander Hoogerstraete, T.; Binnemans, K.; Sun, Z.; Sietsma, J.; Yang, Y. Selective Extraction of Rare-Earth Elements from NdFeB Magnets by a Room-Temperature Electrolysis Pretreatment Step. *ACS Sustainable Chem. Eng.* **2018**, *6*, 9375−9382.

(13) Kitagawa, J.; Uemura, R. Rare Earth Extraction from NdFeB Magnet Using a Closed-Loop Acid Process. *Sci. Rep.* **2017**, *7*, 8039.

(14) Liu, F.; Liu, Z.; Li, Y.; Wilson, B. P.; Lundström, M. Recovery and Separation of Gallium(III) and Germanium(IV) from Zinc Refinery Residues: Part I: Leaching and Iron(III) Removal. *Hydrometallurgy* **2017**, *169*, 564−570.

(15) Abdel-Ghafar, H. M.; Abdel-Aal, E. A.; Ibrahim, M. A. M.; El-Shall, H.; Ismail, A. K. Purification of High Iron Wet-Process Phosphoric Acid via Oxalate Precipitation Method. *Hydrometallurgy* **2019**, *184*, 1−8.

(16) Malmary, G.; Faizal, M.; Albet, J.; Molinier, J. Liquid-Liquid Equilibria of Acetic, Formic, and Oxalic Acids between Water and Tributyl Phosphate + Dodecane. *J. Chem. Eng. Data* **1997**, *42*, 985−987.

(17) Barnes, N. G.; Gramajo de Doz, M. B.; Sólimo, H. N. Liquid−Liquid Extraction of Oxalic Acid from Aqueous Solutions with Tributyl Phosphate and a Mixed Solvent at 303.15 K. *J. Chem. Eng. Data* **1999**, *44*, 430−434.

(18) Tian, Q. H.; Li, Z. H.; Guo, X. Y. Selective Extraction of Oxalic Acid from Cobalt Mother-Liquor with Complexing Agent P350. *J. Cent. South Univ.* **2009**, *40*, 884−890.

(19) Yang, Y.; Wang, X.; Wang, M.; Wang, H.; Xian, P. Recovery of Iron from Red Mud by Selective Leach with Oxalic Acid. *Hydrometallurgy* **2015**, *157*, 239−245.

(20) Luque-García, J. L.; Luque de Castro, M. D. Ultrasound: A Powerful Tool for Leaching. *TrAC, Trends Anal. Chem.* **2003**, *22*, 41−47.

(21) Du, F.; Li, J.; Li, X.; Zhang, Z. Improvement of Iron Removal from Silica Sand Using Ultrasound-Assisted Oxalic Acid. *Ultrason. Sonochem.* **2011**, *18*, 389−393.

(22) Xin, W. A. N. G.; Srinivasakannan, C.; Xin-hui, D. U. A. N.; Jin-hui, P.; Da-jin, Y.; Shao-hua, J. Leaching Kinetics of Zinc Residues Augmented with Ultrasound. *Sep. Purif. Technol.* **2013**, *115*, 66−72.

(23) Zhang, L.; Guo, W.; Peng, J.; Li, J.; Lin, G.; Yu, X. Comparison of Ultrasonic-Assisted and Regular Leaching of Germanium from by-Product of Zinc Metallurgy. *Ultrason. Sonochem.* **2016**, *31*, 143−149.

(24) Liu, F.; Liu, Z.; Li, Y.; Wilson, B. P.; Lundström, M. Extraction of Ga and Ge from Zinc Refinery Residues in $H_2C_2O_4$ Solutions Containing H_2O_2. *Int. J. Miner. Process.* **2017**, *163*, 14−23.

DOI: 10.1021/acssuschemeng.9b04351
ACS Sustainable Chem. Eng. 2019, 7, 17372−17378